ELSEVIER

Nuclear Instruments and Methods in Physics Research A 399 (1997) 477–488

NUCLEAR INSTRUMENTS & METHODS IN PHYSICS RESEARCH Section A

Experimental beam test of the SilEye2 apparatus

V. Bidoli [a], M. Casolino [a], M. De Pascale [a], G. Furano [a], A. Morselli [a,*], P. Picozza [a], E. Reali [a], R. Sparvoli [a], A. Galper [b], Yu. Ozerov [b], A. Popov [b], V. Zemskov [b], V. Zverev [b], A. Alexandrov [c], S. Avdeev [c], V. Shabelnikov [c], M. Boezio [d], P. Carlson [d], C. Fuglesang [e,1], G. Barbellini [f], W. Bonvicini [f], A. Vacchi [f], N. Zampa [f], S. Giuntoli [g], G. Mazzenga [g], M. Ricci [g], P. Spillantini [h],

[a] *Department of Physics, II University of Rome "Tor Vergata" and INFN, Italy*
[b] *Moscow State Engineering Physics Institute, Moscow, Russia*
[c] *Russian Space Corporation "Energia" by name Korolev, Korolev, Moscow region, Russia*
[d] *Royal Institute of Technology, Stockholm, Sweden*
[e] *European Space Agency, EAC, Cologne, Germany*
[f] *Department of Physics, University of Trieste and INFN, Italy*
[g] *I.N.F.N Laboratori Nazionali, Frascati, Italy*
[h] *Department of Physics, University of Firenze and INFN, Italy*

Received 25 June 1997

Abstract

We present the experimental results obtained with the SilEye2 apparatus during one week test run at the Svedberg Laboratory, Sweden. These results will be used for energy calibration of the data collected on board the MIR Space Station from fall 1997. Data that will be collected with SilEye2 are necessary to understand the phenomenon of optical light flashes (LF) in cosmonauts' eyes during orbital flights and for investigation of the nuclear fluxes in cosmic rays.

1. Introduction

Since the Apollo missions it is known that the crews, after some minutes of dark adaptation, observed brief flashes of white light or pencil-thin streaks of light. The first observation was reported by E. Aldrin during the Apollo 11 mission [1]. Other observations were later reported by Apollo-Soyuz [2]. The frequency of LF depends on orbit parameters, especially on the latitude and grows in polar areas and in the area of the South Atlantic Anomaly. LF are practically absent on the equator, where the charged particles' flux is at minimum. There are different hypothesis on the generation mechanisms of visual effects, like direct interaction of charged particles with the retina of the eye by ionization [3] or Cherenkov effect in the ocular bulb [4] or indirect effect from proton knocked out by protons [5]. It was also suggested that scintillation in the eye lens could cause the observed LF [6]. For a review see [7]. To test this hypothesis we prepared two detectors; the first one is presently on board MIR

* Corresponding author. Tel.: +39 6 7259 4506; fax: +39 6 2025364; e-mail: morselli@roma2.infn.it

[1] Also visiting Royal Institute of Technology.

0168-9002/97/$17.00 © 1997 Elsevier Science B.V. All rights reserved
PII S0168-9002(97)00938-8

Space Station and we already presented preliminary results [8] and the second is scheduled for launch in fall 1997.

2. Technical description of the SilEye apparatus

2.1. General overview

The SilEye detector is a unique device. It can measure particle energy losses from 2.5 Minimum Ionizing Particles (MIPs) to 2500 MIPs (we take 1 MIP = 105 keV) and determine the coordinates of traversing particles with an accuracy of ±1.8 mm and an angular accuracy of 3.3°. This instrument can be used for cosmic rays studies, medical-biological and technological space researches.

It can be seen as a completely software-controlled solid-state detector; its principle characteristics are: small dimensions, portability and low power consumption, user-friendly interface, real-time data analysis. During the future on board MIR session, the apparatus can detect in real time the passage of particles which traverse the eyes and register on the on-board computer the six coordinates and energy depositions from which the direction and properties of the particles can be determined. Time of LF occurrence seen by the astronauts are also stored in a separate file for off-line correlation. The system monitors also astronaut's dark adaptation and reaction time and performs reliability controls on device performances. The astronaut uses a joystick to register light flashes in order to minimize reaction time. All the physic parameters of the detector (like gain or threshold) are completely software-controlled. LEDs were added inside the astronaut's mask to check eye–detector alignment, minimum level of astronauts light sensitivity and readiness. The maximum acquisition rate is not lower than 60 Hz.

2.2. Detector and front end electronics

The SilEye2 apparatus benefits of the technological developments made for the NINA calorimeter [9]. The main body of our detector consists of six silicon views. A view is made of a square ($6\times6\,cm^2$) wafer of silicon, divided in 16 strips, each 3.6 mm wide. Two views, orthogonally attached, constitute a plane. We have three planes for a total number of 96 strips. The distance between the silicon planes is 14 mm. Each silicon strip is 380±15 μm thick, giving a total active thickness of 2.3 mm. The silicon strips act like completely depleted p–n junctions, and need to be supplied by a DC tension of 36 V, obtained by batteries, to completely disconnect the silicon power supply from the electronics power supply. Not all strips are read as physical data; strips 1 and 16 of planes 2 and 3 are connected together and their sum value is read; strips 1 and 16 of plane 1 are disconnected. In this way we have (14+1)*4+14*2 = 88 data words from the strips. We have also 8 housekeeping data words: 3 current meters for the 3 planes, 2 Analog Low Rate Meter (up to 400 Hz) for plane 1 (X and Y view), 1 Analog High Rate meter per plane (up to 20 kHz). In total there are 96 data words per event. Each pair of silicon views is mounted on a ceramic border with appropriate electrical contacts. The Front-End board consists of the silicon planes and of the analogic preamplifiers. The analog signal from the Front-End board goes through the connector to the Read-out Board. Both the electronic boards are mounted on aluminum frames which are 1.5 cm tall, 1.5 mm thick and have appropriate holes to assemble the apparatus in vertical position. When the frames are mounted, they constitute a good shield against light coming from the sides and also protect silicon and electronics. The current signals coming from the silicon strips are very fast (less than 40 ns) and very weak (in electrons 1 MIP = $30400e^-$ = 4.86 fC). These signals go into charge preamplifiers and then into shaping amplifiers that prepare them for sample and hold.

2.3. Read-out

All analog signals from the strips come into the Read-out board. This board has the same shape as the Front-End boards. It performs the Analog-to-Digital conversion of data, trigger functions and telecommands probe. A multiplexer scrolls all the strips and gives the appropriate signal to the ADC, that converts the analog signal to a 12-bit (4096 ADC Ch.) word. The ADC has a dynamic range from 2.5 up to 2500 MIPs (12.2 pC), corresponding to 0.61 MIP/ch.

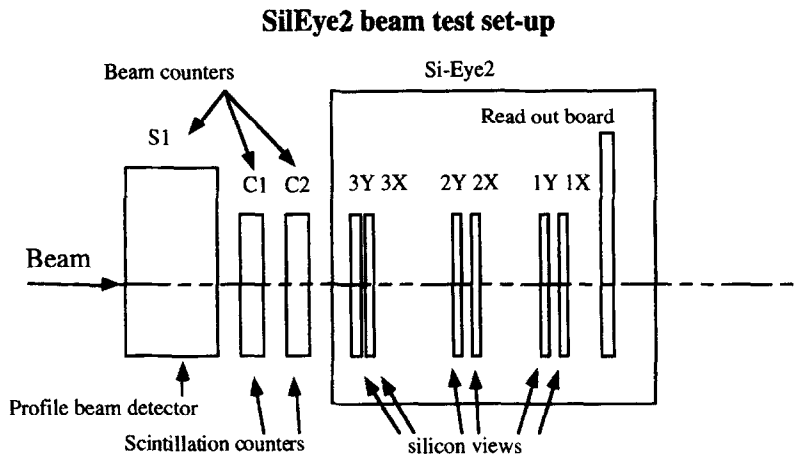

Fig. 1. Beam test set-up.

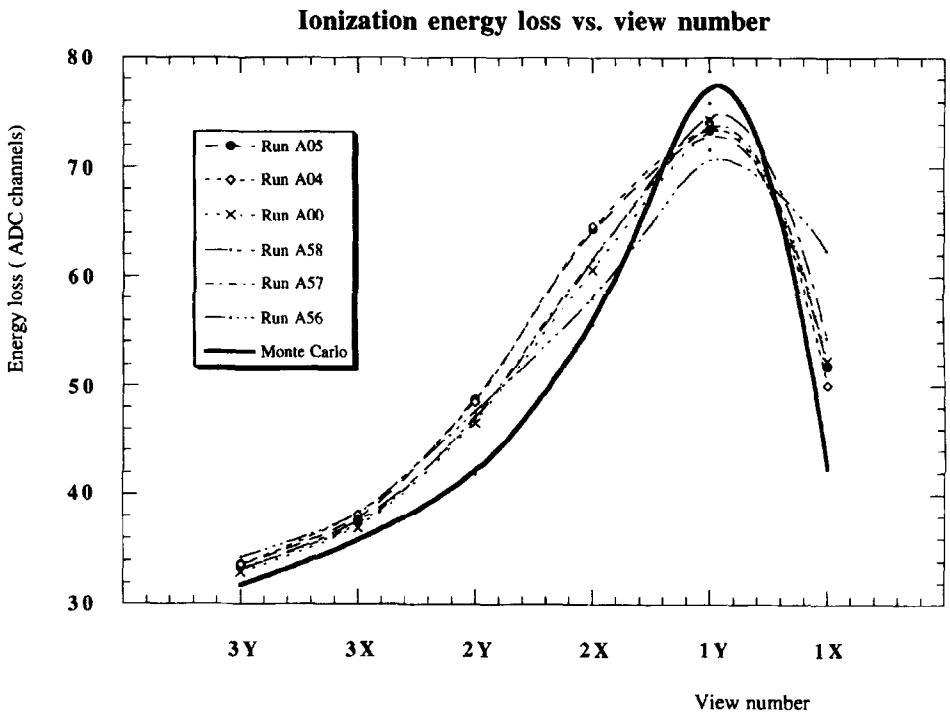

Fig. 2. Ionization energy loss versus view number for six different runs (at 20 MeV in the first view). Comparison of data and Monte-Carlo simulation (the Monte Carlo takes into account all the material in front of the detector).

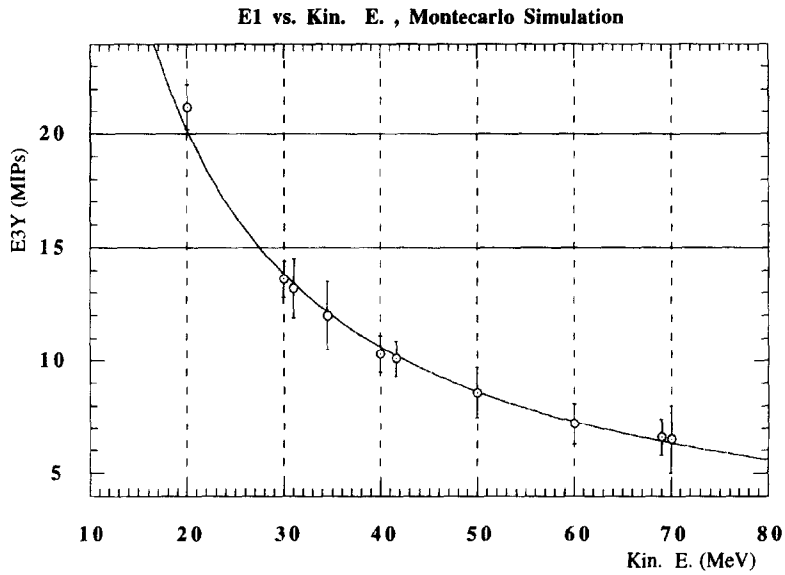

Fig. 3. Monte-Carlo simulation of the energy loss (in MIP, 1 MIP = 105 keV) in the first view, for different particle kinetic energies

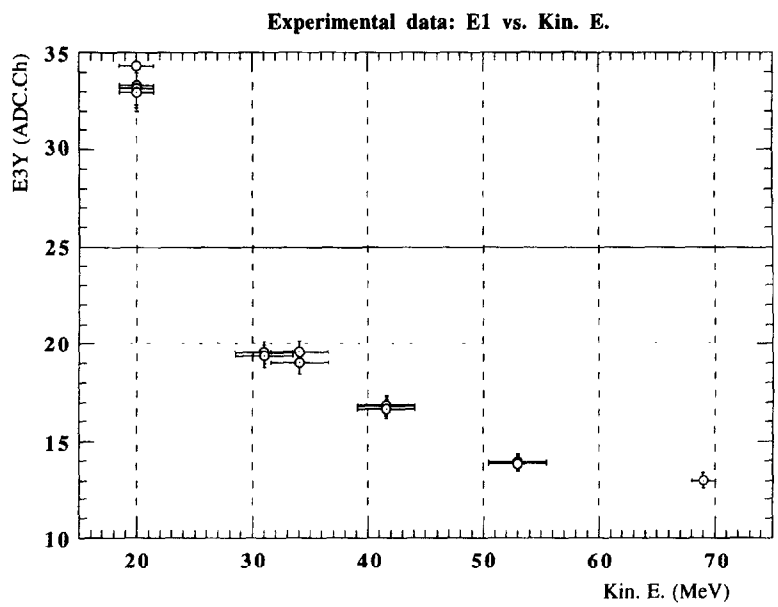

Fig. 4. Experimental results for number of ADC channels versus incoming particle kinetic energies in the first encountered view.

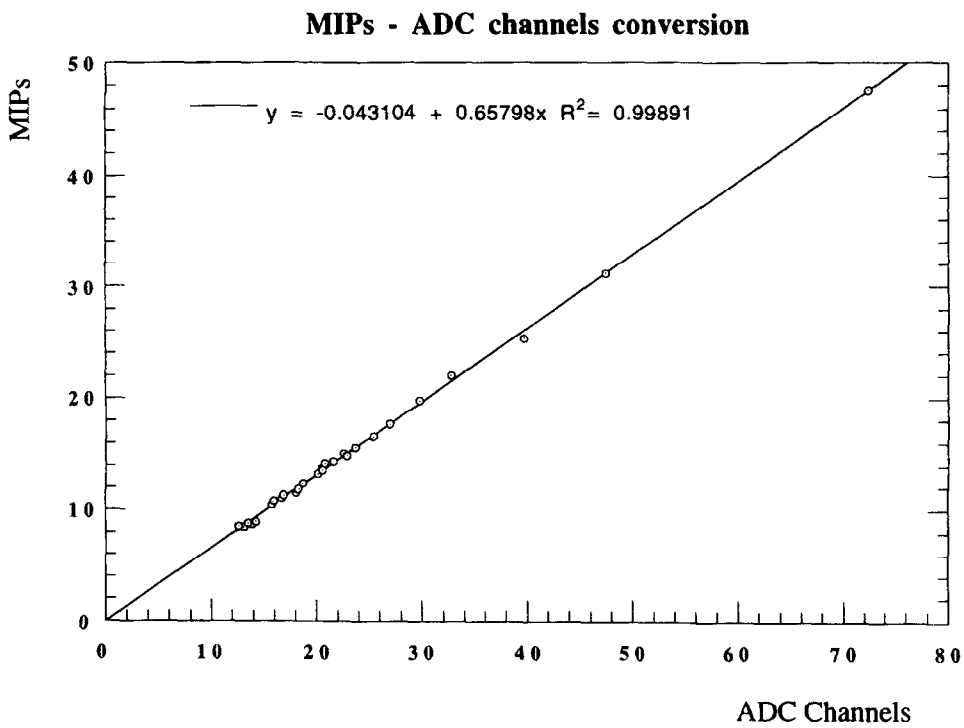

Fig. 5. MIPs versus number of ADC channels for all the runs (different energies and absorber thicknesses).

2.4. Trigger system and threshold

Before being converted, the analog signal goes into a logical comparator that performs triggering operations; two kinds of triggers are available, by changing the appropriate telecommand. Denoting with X1 and Y1 the views of the first plane and with 2 the OR between X2 and Y2, the first (main) trigger is ((X1 AND 3) AND (Y1 OR 2)), the second (spare) trigger is (Y1 AND 3). Triggering logic and telecommand recognizing is performed by a PAL unit mounted on the board. In these tests we used an external trigger coming from scintillators, so both these procedures were passed by.

To discriminate low-level signals it is possible to set a hardware threshold for the sum of all the strips in each view on an analog comparator. For these tests this threshold was set to 200 mV = 2.5 MIP. Telecommands can run various device functions: calibration, triggering, signal amplification, signal hold. The threshold can be set up to 75 MIPs and this feature is very useful to avoid saturation in SAA, the maximum acquisition rate is higher than 60 Hz. Telecommands logical signals come from the computer through the interface board.

From the ADC the digital signal goes into a buffering-FIFO system and can be read by computer.

2.5. Interface

The interface board's main task is to distribute logical signals from and to the acquisition board, to optically decouple them and perform delays in some power supply circuits. The interface board also performs acquisition with external triggers. This board was completely projected and built in INFN laboratories.

2.6. DAQ-Card and User Software

All the I/O communications use the National Instruments DAQ-Card 1200 that allows 24 digital I/Os, 3 wave form outputs, 6 analog I/Os and is fully user-programmable with C++.

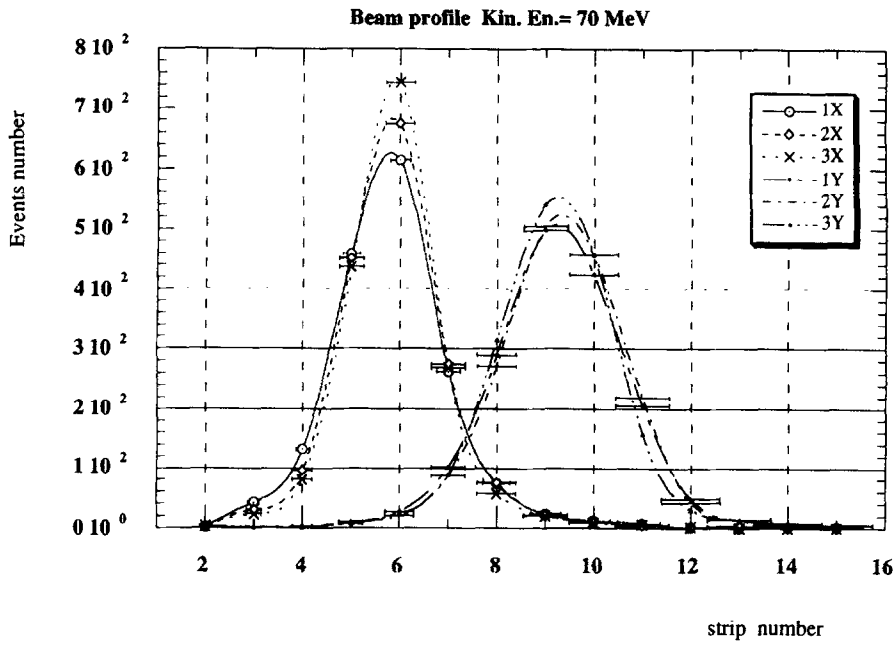

Fig. 6. Beam profile for proton energy of 70 MeV. This figure together with the next one illustrate the possibility of our device to determine the coordinates of the passing particles.

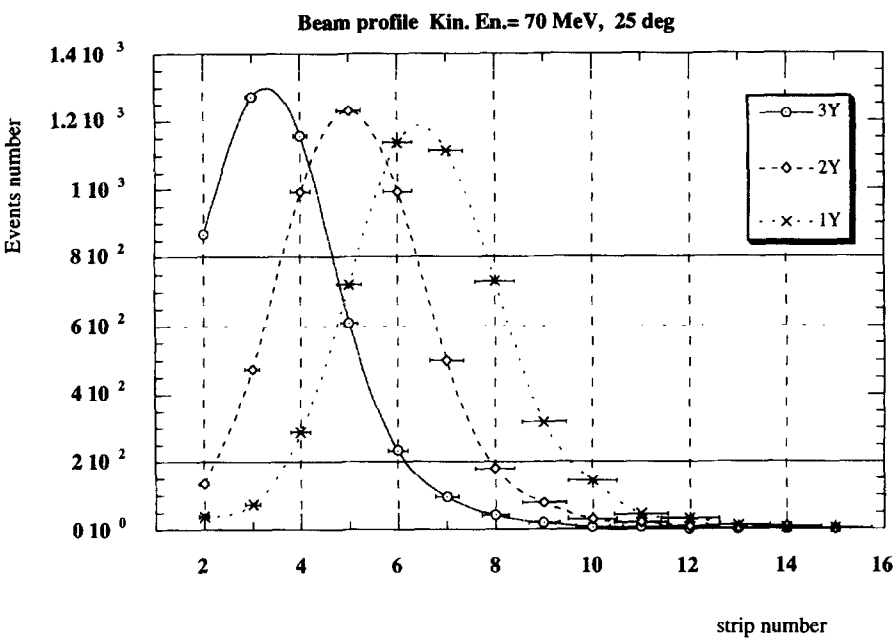

Fig. 7. Beam profile for proton energy of 70 MeV, 25° of silicon planes inclination in Y direction.

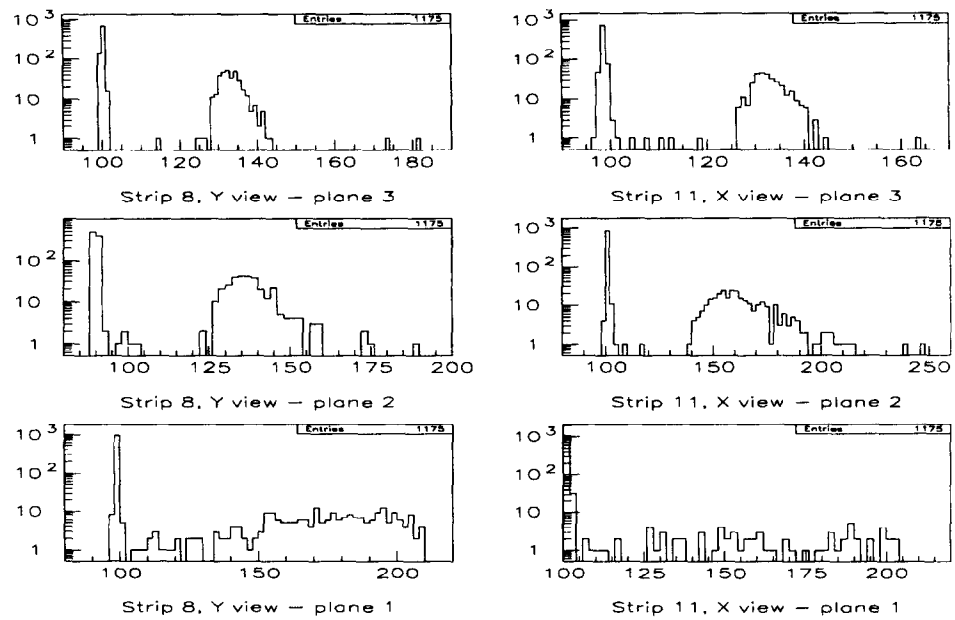

Fig. 8. Energy loss in the different views for run 58 (at 20 MeV in the first view) without pedestal subtraction for single strips so one can see the degree of separation between signal and pedestal.

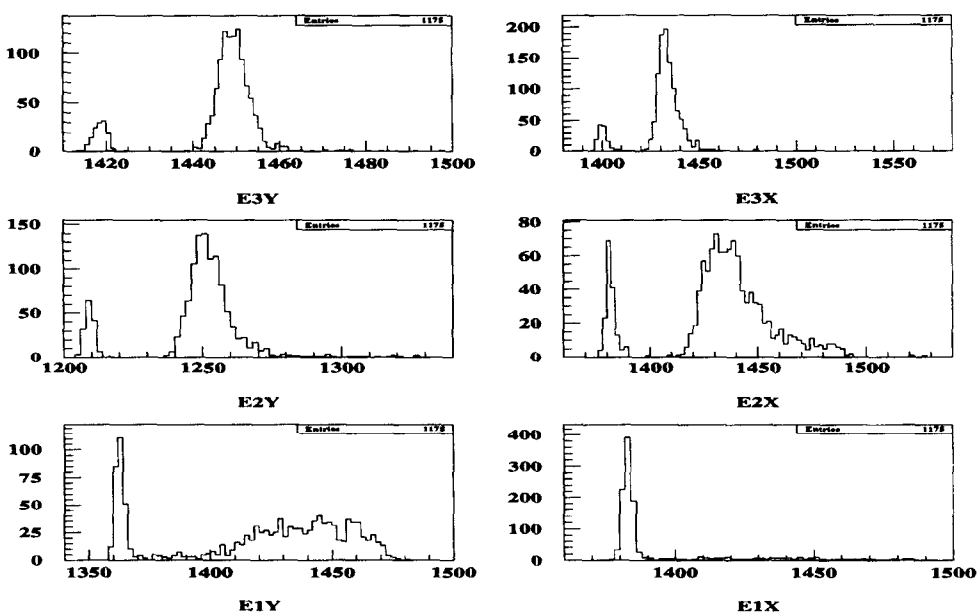

Fig. 9. Energy loss in the different views for run 58 (at 20 MeV in the first view) without pedestal subtraction for the sum of all the strips.

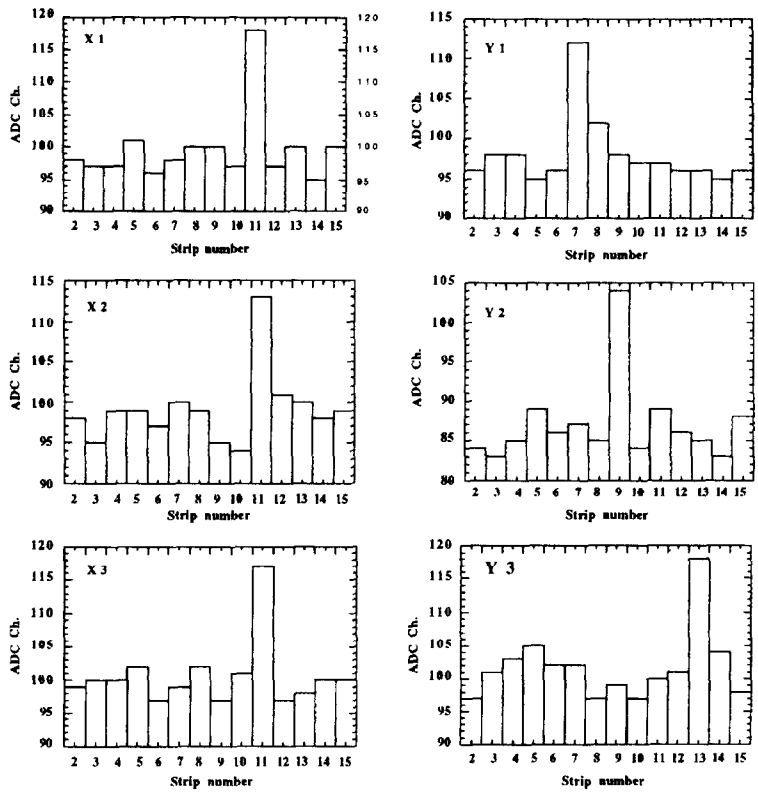

Fig. 10. Energy loss in the different views for a single particle for run 10 (at 25° degrees of inclination in the Y direction and without pedestal subtraction).

The I/O system is connected with an IBM Thinkpad 750C laptop computer. The user interface comprehends a main acquisition program and some fast-analysis routines. The acquisition procedure itself requires a laplink-controlled laptop computer that remains in the beam room. By software it is possible to control almost all device parameters and functions, like trigger, signal amplification, calibrations. The system also controls the handshaking signals like data ready and read-data involved in FIFO discharging.

3. Calibration and control of the device

When started, the device performs an automatic calibration in three steps: pedestal acquisition, noise test, charge injection test. In the first one the system automatically acquires 1024 measurements in standard amplification conditions. The mean values for each channel of these lectures (in number of ADC channels) are taken as pedestal values for each strip and give the mean values of the noise of each strip. The calculated root mean square (RMS) values are taken to set a software threshold to cut pedestal values and noises during acquisition of the events. We take as threshold the value of the pedestal plus 3 RMS. We expect fixed pedestals, whose values can vary only slightly depending on working temperature. To understand the evolution of the silicon strip behavior and of its noise with time, it is necessary to use the pedestals amplified 32 times as noise data. Now we have a conversion factor of (2500/32) MIP/4096 ch = 0.019 MIP/ch that means a charge of 3/32–0.1 fC/ch. With these values we can do a better analysis on the silicon behavior and defects.

Amplification lines can give gain factors that may differ of $\pm 10\%$ between channels. This problem,

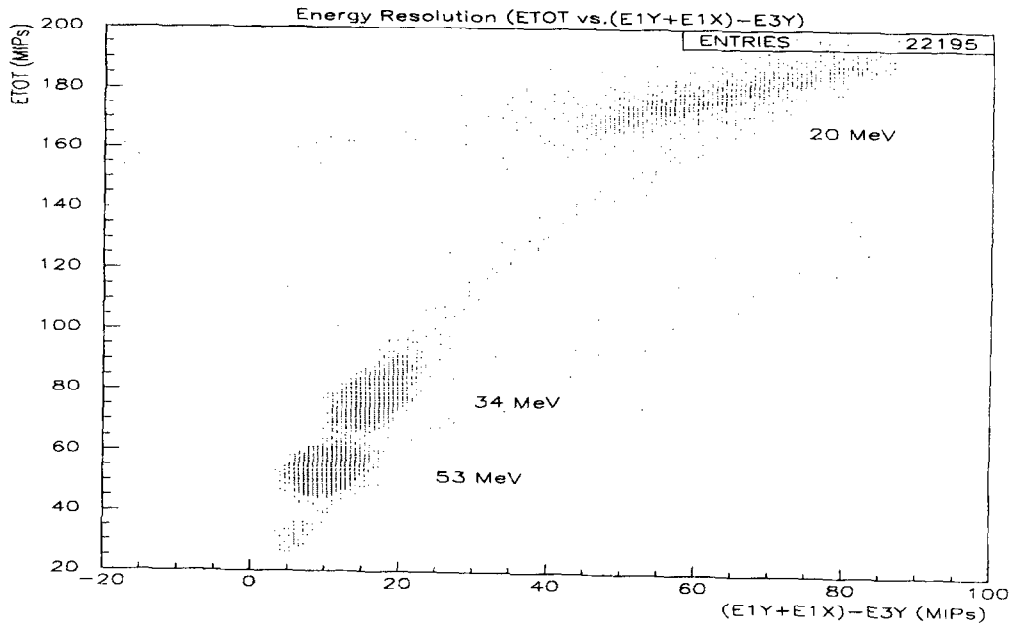

Fig. 11. Distibution of the total detected energy versus the difference between the energy loss in the last plane and in the first view.

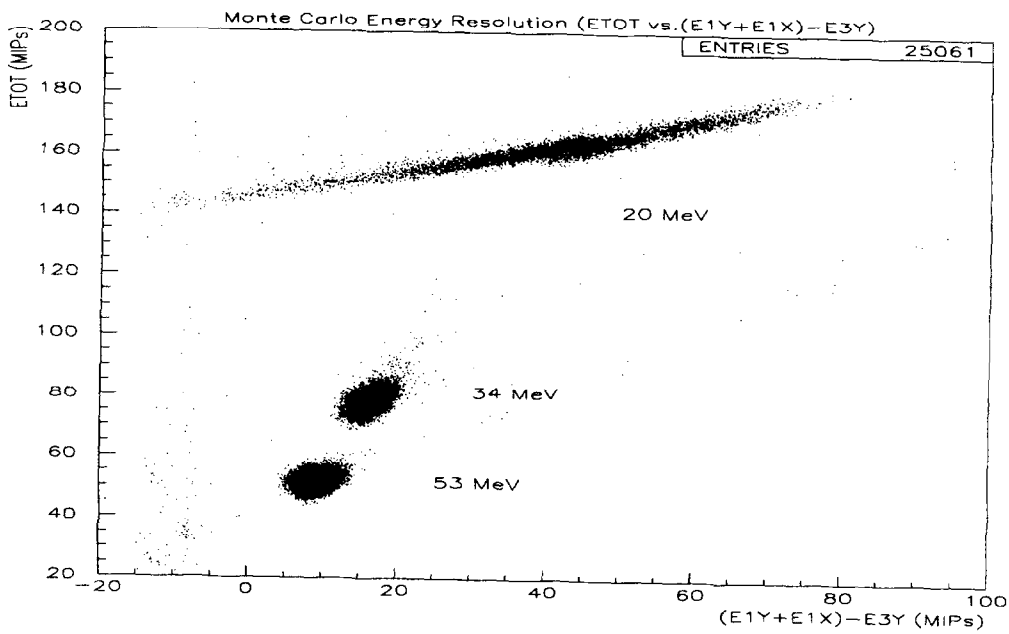

Fig. 12. Simulated distibution of the total detected energy versus the difference between the energy loss in the last plane and in the first view

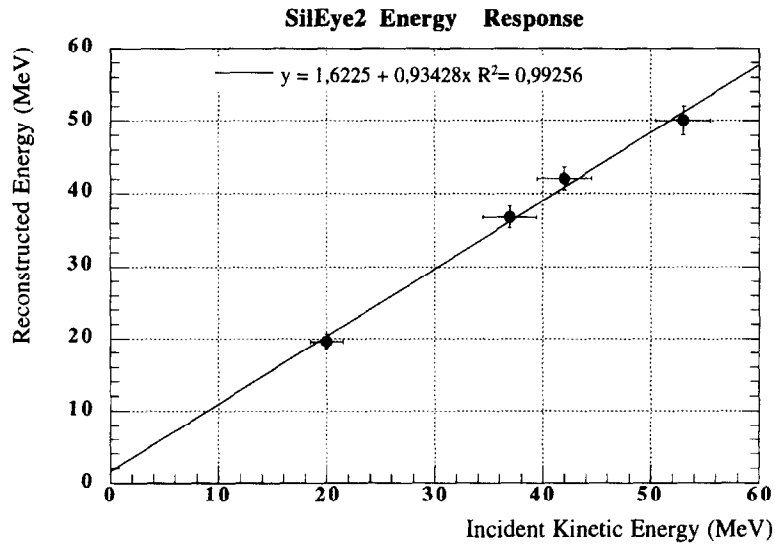

Fig. 13. Energy response of SilEye2 as a function of reconstructed proton energy.

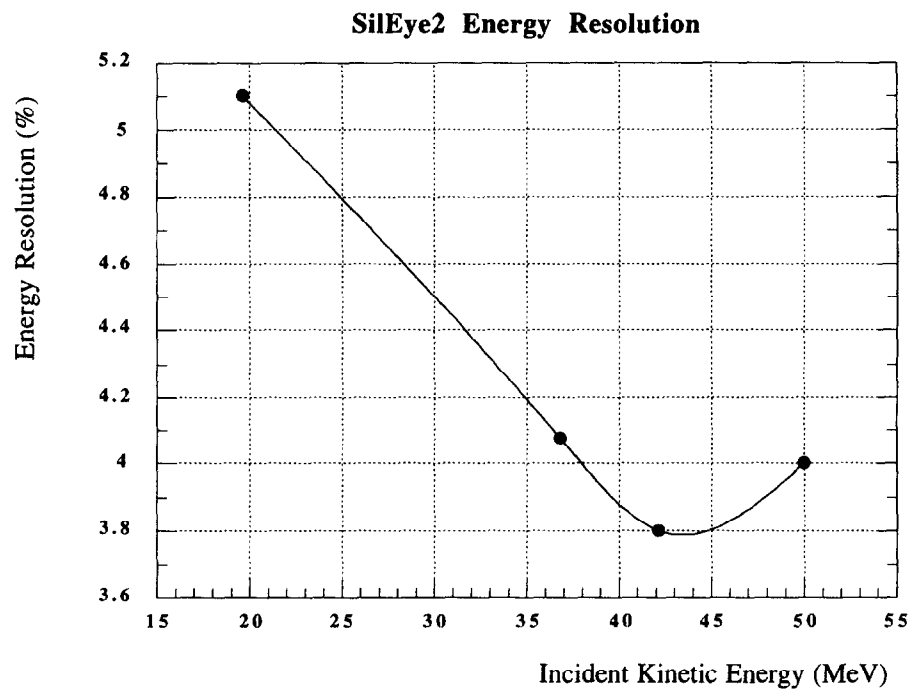

Fig. 14. Energy resolution (RMS/E) of SilEye2 as a function of reconstructed proton energy.

together with the importance of having a system to control variations in the electronics device, required the realization of a calibration system with the injection of a known charge on the channel in order to build linearity curves for each channel. Injection capacitors have a weighted value of 4.7 pF, so for a charge injection tension value of 1 mV we will have an injected charge of 4.7 fC (nearly 1 MIP). From software is possible to choose the voltage for charge injection in all the dynamic range of the ADC. For normal working tests we choose 4 values for tension : 0.25, 0.5, 1 and 2 Vs.

3.1. Technical procedures

In the final version, SilEye2 will be equipped with a switching DC-DC converter supply board. For these tests we used 3 AC–DC stabilized power supplies. The system needs 3 different tensions: 2 analog (+6.30 V, 140 mA, −6.3 V, 80 mA), and 1 digital (+5.10 V, 180 mA).

4. Beam test performances

The calibration of the device SilEye2 was carried out on a proton beam from the CELSIUS storage ring at TSL, Uppsala. The measurements were done at two different proton energies: 48 and 70 MeV. The device was placed at a distance of about 25 cm from the vacuum tube with a profile detector and two scintillation counters in front. The thickness of the total material in front of the detector is equivalent to 1.57 cm of plastic scintillator (see Figs. 1 and 2). In a 70 MeV run, the two scintillation counters were placed behind the device. In the 48 MeV runs protons stop in the 5th or 6th silicon detector with big energy losses up to 50 MIP. This feature is very useful for us, because the device is intended for investigations of low energy protons and nuclei in cosmic rays. The main part of the calibration stages was performed with orthogonally incident particles. One 48 MeV run was performed with an inclination of 5° and two 70 MeV runs were performed at 25°. Additional external aluminum absorbers were installed in front of SilEye2 instrument during some 70 MeV runs with thicknesses of 4, 6.1 and 7 mm. Three runs with different values of aluminium absorbers were performed.

5. Results

We have simulated, with standard Geant 3.21 Monte-Carlo program, all the beam conditions with different energies and absorbers. To obtain the calibration curve of Fig. 5 we compared the monte-carlo simulation (Fig. 3) with the experimental data (Fig. 4). The points in Fig. 4 at 53, 42, 34 and 31 MeV were obtained during the 70 MeV runs with 0, 4, 6.1, and 7 mm absorber thickness respectively and scintillation counters in front of the device. The point at 69 MeV was obtained with scintillation counters behind the device. The point at 20 MeV was obtained during the 48 MeV run with scintillation counters only in front of the device. The value for the ratio MIPs/ADC Ch. is 0.66±0.06, in good agreement with the theoretical value. In Fig. 6 and 7, we show the beam profile on the three planes for orthogonally incident beam and 25° angled beam. In Fig. 8 the energy loss sum for a single strip and all the events of run 58 (a 48 MeV run) are shown as an example of separation between pedestals and particle energy loss profiles. In this run 48 MeV particles stop in the 5th view, releasing the maximum amount of energy. Fig. 9 is the same plot for the sum of all the strips. In Fig. 10 is shown the energy loss in the different views for a single particle for run 10 (at 53 MeV, 25° of inclination). In Fig. 11 the distribution of the total detected energy versus the difference between the energy lost in the last plane and in the first view is plotted. It can be seen that the protons' energies are very well separated, although not so well as in the Monte-Carlo simulation (Fig. 12) because at these energies very little differences in the crossed thickness of the material in front of the detector give big differences in the deposited energies. In Figs. 13 and 14 are plotted the energy response and the energy resolution (RMS/E) of SilEye2 as a function of reconstructed proton energy for events with straight tracks in both views which have declination of middle point in both views no more than one strip from the fitted line. Events with two or more hitted strips in one layer were excluded. The response of SilEye2, in this energy range, shows a quasi-linear behaviour.

6. Conclusion

Although with a weight of less than 5 Kg and power consumption less then 7 W (at 27 V), the SilEye2 apparatus has demonstrated to be able to detect in real time the passage of particles which traverse the eyes and register on the on-board computer the six coordinates and energy depositions from which the direction and properties of the particles can be determined. We have shown that protons' energy resolution is better than 6% for proton kinetic energies higher than 20 MeV. Nuclei discrimination is under examination and it will be presented elsewhere. Time of LF occurrence can also be stored in a separate file for off-line correlation.

This apparatus will be very useful for the understanding of the phenomena of optical light flashes as well as for the study of the level and the composition of cosmic rays on board MIR station.

Acknowledgements

We wish to thank the people of LABEN, who built the front-end and the read-out board, for their effort and special interest in this experiment. We wish to give special thanks to the mechanic and the control beam people at the Svedberg laboratory accelerator in Uppsala for the help on the mechanical set up and the definition of the beam parameters. They allowed a successful test.

References

[1] W.Z. Osborne, L.S. Pinsky, J.V. Baily, Apollo light flash investigations, Biomedical results of Apollo NASA SP-368, 1975, pp. 355–365.
[2] T.F. Budinger, C.A. Tobias, R.H. Huesman et al., Light flash observations, Experiment mA-106, Apollo-Soyuz Test Project Summary Science Report, NASA SP-412, pp. 193–208.b
[3] R.A. Hoffman, L.S. Pinsky, W.Z. Osborne, J.V. Baily, Visual light flash observation on Skylab 4, Biomedical results from Skylab, NASA SP-377, 1977, pp. 127–130.
[4] G.G. Fazio, J.V. Jelley, W.N. Charman, Nature 228 (1970) 260–264.
[5] J. Fremlin, New Scientist 47 (1970) 42.
[6] I. MacAulay, Nature 232 (1971) 421.
[7] G. Horneck, Nucl. Tracks Radiat. Meas. 20 (1) (1992) 188.
[8] A. Galper et al., SilEye on MIR – first active detector for the study of Light Flashes in space, Proc. 6th European Symposium on Life Sciences Research in Space, 17–21 June, Trondheim, Norway, 1996.
[9] G. Barbiellini et al., A satellite born charged particle telescope for the study of cosmic ray nuclei, XXIV Internat. Cosmic Ray Conf., OG 10.3.11, vol. 3, Roma, 1995, p. 607.